Near-Optimal PLL Design for Decision-Feedback Carrier and Timing Recovery

Oded Yaniv, *Senior Member, IEEE*, and Dan Raphaeli, *Senior Member, IEEE*

***Abstract*—A new design method is presented for the design of PLL loop filters for carrier recovery, bit timing, or other synchronization loops given the phase noise spectrum and noise level. Unlike the conventional designs, our design incorporates a possible large decision delay and S-curve slope uncertainty. Large decision delays frequently exists in modern receivers due to, for example, a convolutional decoder or an equalizer. The new design also applies to coherent optical communications where delay in the loop limits the laser linewidth. We provide an easy-to-use complete design procedure for second-order loops. We also introduce a design procedure for higher order loops for near-optimal performance. We show that using the traditional second-order loop is suboptimal when there is a delay in the loop, and also show large improvements, either in the amount of allowed delay, or the phase error variance in the presence of delay.**

I. Introduction

THE phase-locked loop (PLL) principle has been successfully used for decades for tracking the carrier phase and the bit timing. First- or second-order loops are sufficient in most cases. Optimal design of PLL without delay in the presence of oscillator phase noise is well known [11], [14]. Most modern communication receivers incorporate coding and/or equalization and/or partial response detectors, and it is advantageous or sometimes necessary to use the output of the decoder or equalizer for data detection before phase or timing error information is produced for the synchronization loop [6], [15], [19], [20]. The decoder and/or equalizer creates delay into the operation of the PLL used for the synchronization, and, for the case when such delay becomes problematic, several authors proposed combined detection and phase tracking, for example [15], [22], or use less reliable tentative decisions [23]. Between the two loops, the major problem is in the carrier tracking loop since it needs to be wide enough to track the oscillator phase noise. The timing loop works at the symbol rate rather than carrier frequency, therefore its phase noise is normally lower and the loop is allowed to be narrow. However, sufficient delay that can be caused by the decoder (for example, a turbo decoder) can be problematic even for timing loops. The problem of loop design becomes complicated when there is a large uncertainty in the phase detector S-curve slope, which translates to uncertainty in the loop gain. Causes for such uncertainty are numerous, such as residual errors after AGC (or no AGC) in mobile receivers or in burst-mode receivers, error rate change in decision feedback loops, timing errors, and intersymbol interference (ISI). Although the implementation of the loop will be digital in most cases, it is convenient to design first an analog loop and then convert the controller to discrete form using standard techniques such as the bilinear transform. In this way, the design is not dependent on the sampling rate chosen, and the approximation is very accurate if the sampling rate is much higher than the loop delay. For example, the sampling rate is the symbol rate, and the loop delay is tens of symbols. The case where the sampling rate is lower than 10/delay is considered in a following paper.

When significant delay is incorporated into the PLL, the second-order loop which is traditionally used is far from being optimal and a new loop filter design is desired. The design presented in this paper is very close to optimal with respect to the mean square error of the phase in the presence of a known delay, phase noise spectrum, requirements for specific gain and phase margins, and given loop gain uncertainty. These margins should be kept for any gain (within the range of uncertainty) of the PLL open loop. These combined design constraints are known in the feedback control community as mixed $\mathrm{H}_2/\mathrm{H}_\infty$ synthesis with output feedback and plant uncertainty.

We use the notation "upper gain margin" for the maximum amount of loop gain which the PLL can lose without losing stability and "lower gain margin" for maximum increase in loop gain without losing stability. Both gain and phase margins ensure fast settling step response and eliminate closed-loop resonances. For third and higher order PLLs, lower as well as upper gain margins are mandatory in order to guarantee the stability of the PLL.

A general treatment of optimal controller design for a loop having only rational transfer functions in the loop is given in [21]. Design of an optimal PLL with pure delay can be executed to an arbitrary accuracy using a Padé approximation of high enough order [9] (a Padé is a rational transfer function approximation of pure delay e^{-sT} which preserves amplitude). The outcome, of course, will be a complex loop filter, but second-order approximation leads to satisfactory results. Unfortunately, for a large delay, the optimal design will not satisfy the margins constraints. The approach taken here to solve the optimization is a design process composed of two steps. The first step is the solution of the optimal controller for PLL with delay when a Padé approximation replaces the delay. The second step is based on the feedback synthesis theory known as QFT [4], [12], [13]. The QFT technique is applied to modify the loop filter designed in the first step to satisfy the margins constraints. Finally, it was

Paper approved by L. Vandendorpe, the Editor for Transmission Systems of the IEEE Communications Society. Manuscript received December 15, 1999; revised May 15, 2000, and November 15, 2000. This paper was presented in part at the IEEE International Conference on Communications (ICC'99), Vancouver, Canada, June 6–10, 1999.

The authors are with the Faculty of Engineering, Department of Electrical Engineering Systems, Tel Aviv University, Tel Aviv 69 978, Israel (e-mail: yaniv@eng.tau.ac.il; danr@eng.tau.ac.il).

Publisher Item Identifier S 0090-6778(01)08170-3.

shown how to design an optimal PI (second-order) loop filter, and it was shown that the optimal loop filter of the PI form is not satisfactory in case of significant delay and/or reasonable gain uncertainty.

The proposed design methodology also suits other fields such as optical communication using coherent detection and RF synthesizers. Although the theory developed here takes place in continuous time, the same approach can be used for a discrete time PLL.

Most of the work on PLLs with delay was done in the framework of optical communications. In [2] the loop filter complexity was bypassed, for the usual laser phase noise spectrum, $\approx 1/f^2$, assuming the loop filter is of the PI form $2\xi\omega_n + \omega_n^2$, and a design technique to calculate the optimal ω_n was presented. In [18], first and second Padé approximations were used to estimate the degradation of the phase noise variance compared to zero delay, and the loop filter again is of the PI form. Treatment of the effect of time delay on the overall phase error variance was also discussed in [10]. Here again, the same simplified PI loop filter was used and the optimal criterion was the parameter ω_n which was calculated numerically. The significance of the loop delay on the stability of discrete time PLLs was discussed quantitatively in [3]. Finally, we would like to mention that loop delay also degrades the PLL loop pull-in range. For a quantitative discussion based on a simple loop filter, see [17]. The structure of this paper is as follows. After the problem statement, an algorithm for a high-order loop will be developed. Next, an independent design procedure is given for loops having the PI form (second-order loops).

II. Statement of the Problem

There are various forms for PLLs; however, without loss of generality, we can treat the basic PLL form used for tracking a sinusoid of frequency ω_0. The PLL model used here is depicted schematically in Fig. 1(a). It consists of a phase detector, loop filter $F(s)$, voltage-controlled oscillator (VCO), and an optional pure delay which represents the undesired effect, for example, of a decision delay in a decision feedback loop. The inputs to the phase detector are two signals: the sum of the carrier with phase modulation or phase noise $\theta(t)$ and noise $n(t)$

$$y(t) = \sqrt{2}A\sin(\omega_0 t + \theta(t)) + n(t)$$

and the VCO output

$$v(t) = \sqrt{2}\cos(\omega_0 t + \hat{\theta}(t)).$$

The output of the phase detector, assuming it includes an appropriate low-pass filter, is

$$e(t) = A\sin(\theta - \hat{\theta}(t)) + n(t).$$

In other forms of PLLs, the function $\sin(x)$ may be replaced with other appropriate functions which are frequently called S-curve functions. When tracking, the PLL can be approximated for small phase errors by the linear model as depicted schematically in Fig. 1(b), and its open loop transfer function is

$$L(s) = A\frac{1}{s}F(s)e^{-sT}. \quad (1)$$

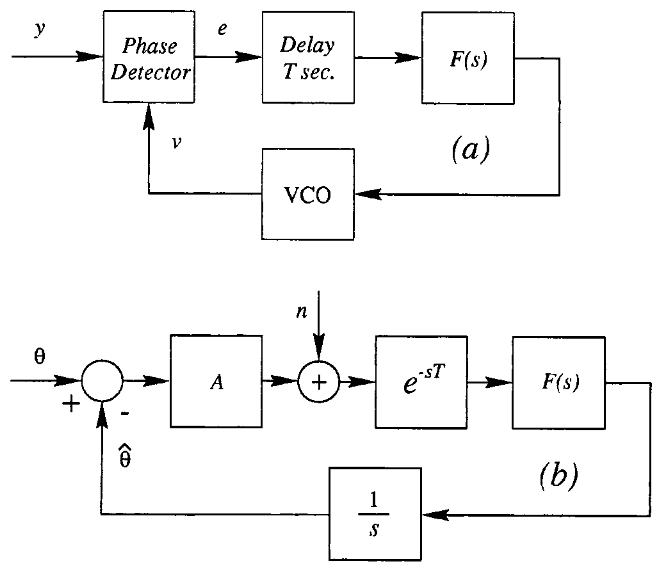

Fig. 1. (a) PLL schematic model and (b) its linear approximation.

Our problem is to design a loop filter $F(s)$ that minimizes the phase error variance σ_e^2, subject to the following data and constraints

- The power spectral density of the noise, n, is $\Phi_n(\omega)$.
- The power spectral density of the phase modulation or phase noise, θ, is $\Phi_\theta(\omega)$. We assume that θ and n are uncorrelated.
- The open loop delay is T.
- The phase detector gain, A, is fixed but only known to belong to an interval $A \in [A_1, A_2]$ where A_1 and A_2 are known (for example, it reflects AGC inaccuracies). Note that if A changes slowly within its allowed interval, the closed-loop response in the time range, where A is about A_0, will be approximately as if $A = A_0$.
- The open-loop response should have some gain and phase margins in order to guarantee a well-damped closed-loop response. These margins are defined here by a constant γ or alternatively by a constant δ such that

$$\left|\frac{L(j\omega)}{1+L(j\omega)}\right| \le \gamma \text{ or } \left|\frac{1}{1+L(j\omega)}\right| \le \delta \quad (2)$$

for all real ω and $A \in [A_1, A_2]$.

The parameter γ determines the gain and phase margins by

$$20\log\frac{\gamma+1}{\gamma}\text{ dB;} \quad 2\sin^{-1}\frac{1}{2\gamma}\text{ deg}$$

and the parameter δ determines the gain and phase margins by

$$20\log\frac{\delta}{\delta-1}\text{ dB;} \quad 2\sin^{-1}\frac{1}{2\delta}\text{ deg.} \quad (3)$$

For example, if $\delta = 1.4$ and there is no gain uncertainty, the guaranteed phase and gain margin are 45° and 10 dB and the guaranteed damping factor (assuming second order model) is 0.4; if one adds 8 dB gain uncertainty (that is, $20\log(A_2/A_1) = 8$), the guaranteed phase margin will not change but the gain margin will be 18 dB for the low A_1 and 10 dB for A_2. For the correlation between the margins, damping ratio and closed-loop time response such as step, overshoot, etc.; see [7].

III. The Proposed Algorithm

The Laplace transform of $e(t)$ is given by

$$e(s) = \frac{\frac{L(s)}{A}}{1+L(s)}n(s) + \frac{1}{1+L(s)}\theta(s)$$

and its variance (assuming zero mean) is

$$\sigma_e^2 = \frac{1}{2\pi}\int_{-\infty}^{\infty}\left|\frac{\frac{L(j\omega)}{A}}{1+L(j\omega)}\right|^2 \Phi_n(\omega)d\omega + \frac{1}{2\pi}\int_{-\infty}^{\infty}\left|\frac{1}{1+L(j\omega)}\right|^2 \Phi_\theta(\omega)d\omega. \quad (4)$$

From now on, for clarity, the factor $(2\pi)^{-1}$ will be omitted. The solution for $F(s)$ which minimizes (4) where the margin conditions are ignored and the pure delay is approximated by a rational transfer function, is a standard stationary filtering problem. For a review and extensions, see [21]. The algorithm which is developed here is based on coprime factorization and controller parameterization [8]. The purpose of the derivations to follow is twofold. It allows us to get the optimal solution, and it allows us to modify the optimal solution in a way that is suitable for the application of the a tool from feedback synthesis theory known as QFT [4], [12], [13] in order to meet the margin conditions while minimizing σ_e^2.

Since σ_e^2 depends on $L(s)$ (and not on its components), we shall incorporate, for simplicity of the representation, the free integrator into $F(s)$. The open loop will then be

$$L(s) = A\tilde{F}(s)e^{-sT}, \text{ where } \tilde{F}(s) = \frac{F(s)}{s}. \quad (5)$$

Let $P(s)$ be a rational transfer function approximation of e^{-sT}. Using the algorithm from [8, ch. 5], we can find polynomial transfer functions $N(s)$, $M(s)$, $X(s)$, and $Y(s)$, such that $P(s) = N(s)/M(s)$ is a coprime factorization over the family of all stable, rational, and proper transfer functions, and $X(s)$ and $Y(s)$ belonging to the same family satisfying

$$N(s)X(s) + M(s)Y(s) = 1.$$

For example, if a first-order Padé approximation is used, that is $P(s) = (1 - sT/2)/(1 + sT/2)$ then $N = (1 - sT/2)/(1 + sT/2)$, $M = 1$, $X(s) = 1$, and $Y(s) = sT/(1 + sT/2)$.

According to the theory found in [8, ch. 5], $\tilde{F}(s)$ stabilizes the PLL if and only if

$$\tilde{F}(s) = \frac{X+MQ}{Y-NQ}\frac{1}{A} \quad (6)$$

where $Q(s)$ is any stable proper and rational function.

Let us denote the spectral factorization of Φ_n/A^2 and Φ_θ by

$$\frac{\Phi_n}{A^2} = \phi_n(s)\phi_n(-s), \quad \Phi_\theta = \phi_\theta(s)\phi_\theta(-s) \quad (7)$$

where $\phi_n(s)$ and $\phi_\theta(s)$ are proper minimum-phase stable transfer functions. Substituting (6) and (7) into (4) gives

$$\sigma_e^2 = \int_{-\infty}^{\infty}|M(Y-NQ)\phi_n|^2 d\omega + \int_{-\infty}^{\infty}|N(X+MQ)\phi_\theta|^2 d\omega. \quad (8)$$

Using the notation $NM = U_{\text{ap}}U_{\text{mp}}$ where U_{ap} is all-pass and U_{mp} stable minimum-phase, the integrand of (8) at $s = j\omega$ reduces to

$$\begin{aligned}
&|MY\phi_n - U_{\text{ap}}U_{\text{mp}}\phi_n Q|^2 + |NX\phi_\theta + U_{\text{ap}}U_{\text{mp}}\phi_\theta Q|^2 \\
&= \left|U_{\text{ap}}^{-1}MY\phi_n - U_{\text{mp}}\phi_n Q\right|^2 + \left|U_{\text{ap}}^{-1}NX\phi_\theta + U_{\text{mp}}\phi_\theta Q\right|^2 \\
&= \left|\left(U_{\text{ap}}^{-1}MY\phi_n\right)_{\text{un}} + \left(U_{\text{ap}}^{-1}MY\phi_n\right)_{\text{st}} - U_{\text{mp}}\phi_n Q\right|^2 \\
&\quad + \left|\left(U_{\text{ap}}^{-1}NX\phi_\theta\right)_{\text{un}} + \left(U_{\text{ap}}^{-1}NX\phi_\theta\right)_{\text{st}} + U_{\text{mp}}\phi_\theta Q\right|^2
\end{aligned} \quad (9)$$

where the subscript un stands for the unstable part of the transfer function and st for its stable part (that is, $x = x_{\text{un}} + x_{\text{st}}$). We use now the observation that in time domain $|x_{\text{un}} + x_{\text{st}}|^2 = |x_{\text{un}}|^2 + |x_{\text{st}}|^2$. This is because by definition x_{un} has only right half-plane poles, thus $x_{\text{un}}(t) = 0$ at $t > 0$, and similarly x_{st} has only left half plane poles, thus $x_{\text{st}}(t) = 0$ at $t < 0$, hence $x_{\text{un}}x_{\text{st}} = 0$, and (9) becomes

$$\begin{aligned}
\sigma_e^2 = &\int_{-\infty}^{\infty}\left(\left|\left(U_{\text{ap}}^{-1}MY\phi_n\right)_{\text{un}}\right|^2 + \left|\left(U_{\text{ap}}^{-1}MY\phi_n\right)_{\text{st}} - U_{\text{mp}}\phi_n Q\right|^2\right) \\
&+ \int_{-\infty}^{\infty}\left(\left|\left(U_{\text{ap}}^{-1}NX\phi_\theta\right)_{\text{un}}\right|^2 + \left|\left(U_{\text{ap}}^{-1}NX\phi_\theta\right)_{\text{st}} + U_{\text{mp}}\phi_\theta Q\right|^2\right) d\omega.
\end{aligned} \quad (10)$$

From (10) it is clear that Q minimizes σ_e^2 if and only if it minimizes (removing terms not depending on Q)

$$\begin{aligned}
\sigma_{e1}^2 &= \int_{-\infty}^{\infty}\left(\left|\left(U_{\text{ap}}^{-1}MY\phi_n\right)_{\text{st}} - U_{\text{mp}}\phi_n Q\right|^2 + \left|\left(U_{\text{ap}}^{-1}NX\phi_\theta\right)_{\text{st}} + U_{\text{mp}}\phi_\theta Q\right|^2\right) d\omega \\
&\stackrel{\text{def}}{=} \int_{-\infty}^{\infty}\left(|a(s) + b(s)Q|^2 + |c(s) + d(s)Q|^2\right)_{s=j\omega} d\omega
\end{aligned} \quad (11)$$

where the last equality is used to define $a(s)$, $b(s)$, $c(s)$, and $d(s)$, respectively. By complex arithmetic, it can be shown that

$$\sigma_{e1}^2(Q) = \int_{-\infty}^{\infty}\left(|\alpha + \beta Q|^2 + |a|^2 + |b|^2 - |\alpha|^2\right)_{s=j\omega} d\omega \quad (12)$$

where $\beta(s)$ and $\alpha(s)$ satisfy the following equations:

$$\beta(s)\beta(-s) = b(s)b(-s) + d(s)d(-s) \quad (13)$$
$$\alpha(-s)\beta(s) = b(s)a(-s) + d(s)c(-s). \quad (14)$$

Equation (13) has power spectral density form, hence $\beta(s)$ is minimum phase and stable. Therefore, the stable $Q(s)$ which minimizes σ_e^2 (also σ_{e1}^2) is the one that minimizes (after removing terms not depending on Q)

$$\sigma_{e2}^2(Q) = \int_{-\infty}^{\infty} \left(|\alpha_{\rm un}|^2 + |\alpha_{\rm st} + \beta Q|^2 \right) d\omega. \tag{15}$$

Since β is minimum phase, its inverse is stable, therefore σ_e is minimum at

$$Q = -\frac{\alpha_{\rm st}(s)}{\beta(s)} \overset{\rm def}{=} Q_{\rm opt} \tag{16}$$

and by (6) at

$$\tilde{F}(s) = \frac{X + MQ_{\rm opt}}{Y - NQ_{\rm opt}} \frac{1}{A} \overset{\rm def}{=} \tilde{F}_{\rm opt}(s). \tag{17}$$

Due to the phase detector gain uncertainty, σ_e^2 depends on the phase detector gain A. Since $L(s) \propto A$, the argument of each integral in (4) in low frequencies is approximately proportional to $1/A^2$, and since in general the spectral density of Φ_θ is concentrated in low frequencies and that of Φ_n is white, we shall assume the following.

Assumption 3.1: The maximum of $\sigma_e^2(A)$ over $A \in [A_1, A_2]$ is $\sigma_e^2(A_1)$.

This assumption means that a solution that minimizes $\sigma_e(A_1)$ subjected to all other constraints is a solution to our problem.

Clearly $\tilde{F}_{\rm opt}(s)$ for $A = A_1$ is the solution we seek only if the closed loop satisfies the gain and phase margin specification for all possible loop gains. However, if the open-loop gain uncertainty is large and/or the desired margins are large and/or the delay is too large compared to the PLL open-loop bandwidth, $\tilde{F}_{\rm opt}(s)$ will not be a satisfactory solution. It might even destabilize the system for some of the possible open-loop gains (most likely for high gains). Our next step is devoted to synthesizing an appropriate $\tilde{F}(s)$ by modifying $Q_{\rm opt}$.

Let us assume that the gain and phase margin specifications are of the form

$$\left| \frac{L}{1+L} \right| = \left| \frac{AP\tilde{F}}{1 + AP\tilde{F}} \right|_{s=j\omega} \leq \gamma, \quad \forall\, A \in [A_1, A_2]. \tag{18}$$

Let us write the desired Q which satisfies the specs at $A = A_1$ as

$$Q = Q_{\rm opt} - \frac{\lambda(s)}{\beta(s)} \tag{19}$$

where $\lambda(s)$ needs to be found. Then, if M, N, X, and Y are the spectral factorization of P, we have (20), shown at the bottom of the page. Hence, inequality (18) reduces to (21), the inequality on the transfer function $\lambda(s)$, shown at the bottom of the page. Moreover, by (15)

$$\sigma_e^2 \left(Q_{\rm opt} - \frac{\lambda(j\omega)}{\beta(j\omega)} \right) - \sigma_e^2 \left(Q_{\rm opt} \right) = \int_{-\infty}^{\infty} |\lambda(j\omega)|^2 \, d\omega \tag{22}$$

where $\sigma_e^2(x)$ means σ_e^2 computed using $Q = x$. Hence, $\sigma_e^2(Q_{\rm opt})$ is less than $\sigma_e^2(Q)$ by the *2-norm* of $\lambda(s)$. Equations (21) and (22) translate our problem into the following constraint optimization problem: find a stable transfer function, $\lambda(s)$, whose *2-norm* is as small as possible that satisfies inequality (21) at all ω. The solution we seek will be $\tilde{F}$ of (6), where Q is defined in (19). This problem can be solved within the framework of the feedback synthesis theory known as QFT [4], [12], [13]. The QFT technique modified to our problem, as stated above, is now described with the help of an example.

A. Example 1

The example parameters are (units are radians and seconds): $\Phi_\theta = 50^2/\omega^4$, $\Phi_n = 0.01^2$, open-loop delay $T = 0.01$ which is approximated by a second-order Padé approximation [9]

$$e^{-sT} \approx \frac{\left(\frac{1-sT}{4}\right)^2}{\left(\frac{1+sT}{4}\right)^2},$$

and AGC gain, A, which can be any value in the interval $A \in [1, 2]$. The margins constraint is of the form $|L/(1+L)| < 3$ dB, which guarantee 45° phase margin and 5-dB gain margin for $A = 2$ and 11 dB for $A = 1$. These margins are about the lowest one can choose for proper PLL operation [16].

For the AGC gain $A = 1$, the optimal filter $F(s)$ calculated by the algorithm described above, is

$$F(s) = \frac{150(s + 33.3)(s + 400)^2}{s(s^2 + 750s + 600^2)}. \tag{23}$$

$$\begin{aligned} \left| \frac{L}{1+L} \right| &= \left| \frac{AN(X + MQ)}{A_1 M(Y - NQ) + AN(X + MQ)} \right| \\ &= \left| \frac{AN(X + MQ_{\rm opt}) - \frac{ANM}{\beta}\lambda(s)}{A_1 M(Y - NQ_{\rm opt}) + AN(X + MQ_{\rm opt}) + \frac{A_1 MN - ANM}{\beta}\lambda(s)} \right| \end{aligned} \tag{20}$$

$$\left| \frac{AN(X + MQ_{\rm opt}) - \frac{ANM}{\beta}\lambda(s)}{A_1 M(Y - NQ_{\rm opt}) + AN(X + MQ_{\rm opt}) + \frac{A_1 MN - ANM}{\beta}\lambda(s)} \right|_{s=j\omega} \leq \gamma, \quad \forall\, A \in [A_1, A_2] \tag{21}$$

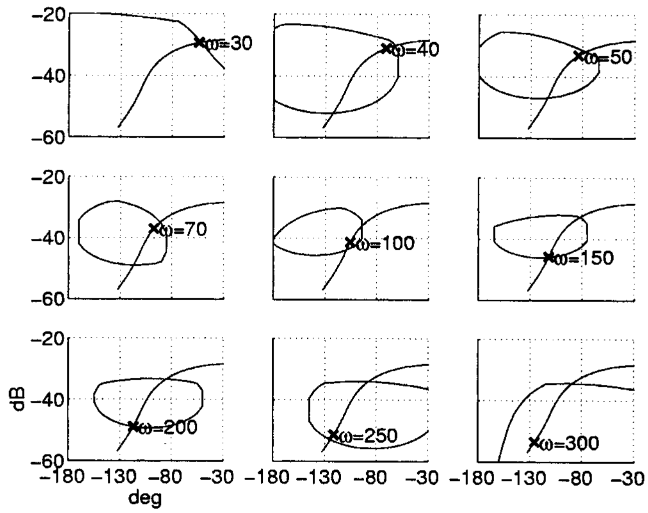

Fig. 2. Complex plane regions for $\lambda(j\omega)$ at some frequencies. The plot of $\lambda(j\omega)$ versus ω is shown and the appropriate $\lambda(\omega)$ is marked by $\times$.

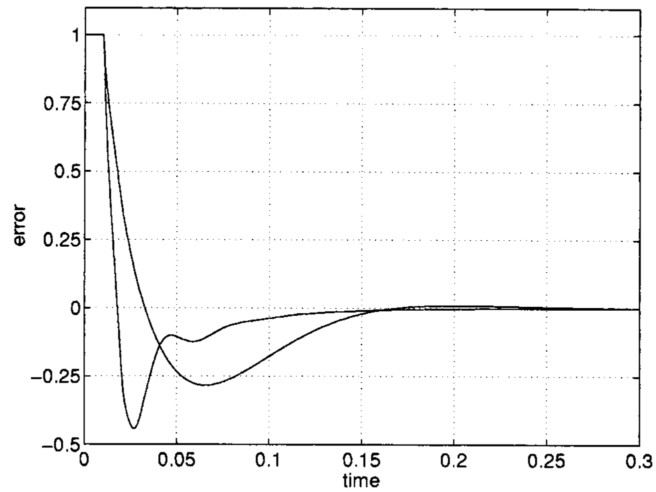

Fig. 3. Time-domain simulation for a phase step, faster response for $A = 2$, slower for $A = 1$.

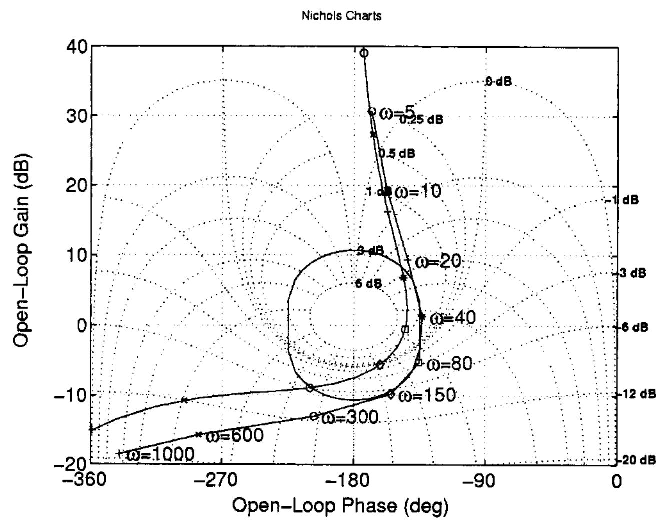

Fig. 4. Comparison between the design $F_r(s)$ which satisfies the margin constraints and the optimal one, $F(s)$, which does not satisfy these constraints.

Using a Bode plot of the open loop $L(s)$ of (1), one can show that the gain and phase margins are approximately 35° and 7.5 dB, respectively, which is 10° and 3.5 dB less than required by the specification $|L/(1+L)| \le \gamma = 3$ dB. The other transfer function is involved in calculating $F(s)$ where

$$X = 1, \quad Y = \frac{sT}{\frac{s^2T^2}{16} + \frac{sT}{2} + 1}$$

$$M = 1, \quad N = \frac{\frac{s^2T^2}{16} - \frac{sT}{2} + 1}{\frac{s^2T^2}{16} + \frac{sT}{2} + 1}$$

$$Q = \frac{s(50-s)}{s^2 + 100s + 5000}, \quad \beta = \frac{0.01s^2}{s^2 + 100s + 5000}.$$

These expressions for $L(s)$, $Q(s)$, and $\beta(s)$ are reduced order (approximations with less poles and zeros of the original designs). Any approximation technique can be used with the criterion of being as close as possible to the norm of $\alpha_{\rm st} + \beta Q$ [see (15)]; the Matlab minreal.m function is an excellent approximation for that purpose. The next step is to design $\lambda(s)$, which is a two-step procedure. First we calculate inequality (21). This inequality on $\lambda(j\omega)$ for each frequency ω and fixed A is a circle in the complex plane using real imaginary coordinates [5]. The intersection of all these circles over all A's in the specified interval $[A_1, A_2]$ is the region in the complex plane in which $\lambda(j\omega)$ is allowed to take values. These regions are shown in Fig. 2 using amplitude and phase coordinates instead of real imaginary coordinates. For example, at $\omega = 70$, $\lambda(j70)$ should be inside the closed curve marked 70; at $\omega = 100$, $\lambda(j100)$ should be inside the closed curve marked 100; and at $\omega = 30$, $\lambda(j30)$ should be below the curve marked 30, which is in fact a closed curve in the real imaginary plane.

The next step is to design $\lambda(s)$ such that $\lambda(j\omega)$ is within the allowed region and its *2-norm* is as small as possible. This process is a trial-and-error process known as loop shaping among the control community. One can start with a second-order transfer function and iterate on its parameters, then add more elements such as lead, lags, etc., until a satisfactory result is obtained. For our example, the shaped $\lambda(s)$ is

$$\lambda(s) = \frac{348(s+70)}{(s+476)(s^2+52s+37^2)}.$$

This designed $\lambda(j\omega)$ appears in each subplot in Fig. 2 and the relative frequencies are marked by $\times$; clearly, at each frequency, it is within its allowed region. After performing model reduction (by canceling close pole/zero pairs), the loop filter is

$$F_r(s) = 140\frac{(s+20)(s+205)}{s(s+700)}.$$

The PLL was simulated for a phase step for $A = 1$ and $A = 2$, and the simulation is shown in Fig. 3.

Fig. 4 compares the open loop $e^{-sT}\tilde{F}(s)$ which was calculated for $A = A_1$ and the open loop $e^{-sT}\tilde{F}_r(s)$ which also satisfies the margin constraints. The comparison uses the Nichols instead of the Bode plot because the phase and gain margins

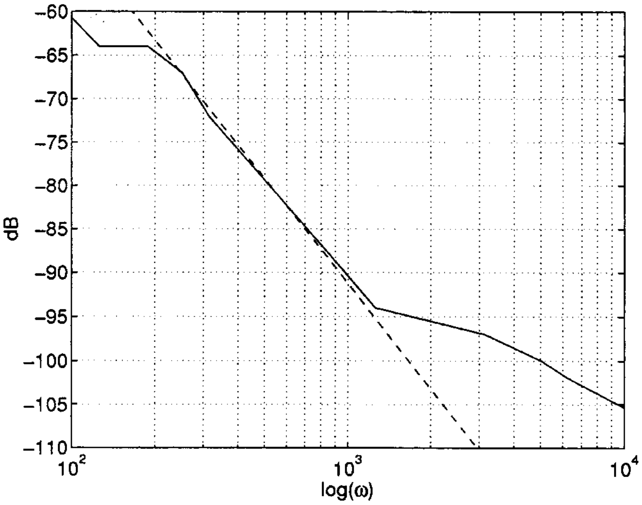

Fig. 5. Phase noise spectral density (solid line) and $\propto 1/\omega^4$ (dashed line).

are easily compared. Also depicted in Fig. 4 is a closed region. This region means that $L(j\omega)$ for $A = A_1$ must be outside it, at all frequencies, in order to satisfy the margin conditions $|AL/(1+AL)| < 3$ dB for all $A \in [A_1, A_2]$. Clearly the solution F_r satisfies the margin constraints while F does not. For $A_1 = 1$, $\sigma_e = 12.8°$, which is 2.8 dB more than the result using the solution which ignores the margin specs and uncertainty $F(s)$ of (23) for which $\sigma_e = 9.1°$. It will be shown in Section IV that, when restricting ourselves to a second-order loop, $F(s) = 31 + 450/s$ and $\sigma_e = 19°$ which is 3.5 dB more than the nonrestricted order design (12.8°).

B. Example 2

This is a practical design example for a coded-modulation system employed by the company HeliOss Communication Inc.,Waltham, MA, who build a very high speed, 155 Mb/s, microwave link at around 30 GHz for transmission of SDH/SONET. They use convolutionally coded QAM modulation. The relevant parameters are as follows. The required minimum average power of the received signal multiplied by the bit duration, E_b, divided by the noise spectral density N_0 (that is E_b/N_0) is 11 dB, and the decoder delay is 77 bits. Assuming that correct symbols are fed back, the normalized noise spectral density is $\phi_n = -93$ dB/Hz. The measured phase noise spectrum is shown in Fig. 5. In the relevant frequency range, it can be approximated by the function $756/w^4$ also shown in Fig. 5. The noise is assumed to be white, and the system delay is $0.5 \cdot 10^{-6}$ s. It is required to design the PLL filter, $F(s)$, such that phase margin of 40° will be guaranteed when the AGC uncertainty can be any value in the interval [1], [2], i.e., 6-dB peak to peak. The optimal solution (ignoring margin constraints) has a gain margin of 9 dB and a phase margin of 38°, which does not satisfy the closed-loop requirements, and the phase error is $\sigma_e = 2.3°$. A design subject to the margins and uncertainty constraints using the technique presented here after model reduction, whose criterion is minimum σ^2 is (s in krad/s)

$$F(s) = 1700\frac{(s+6150)(s+4740)(s+1180)(s+220)}{s^2(s+538)(s^2+15\,350s+11\,100^2)}$$

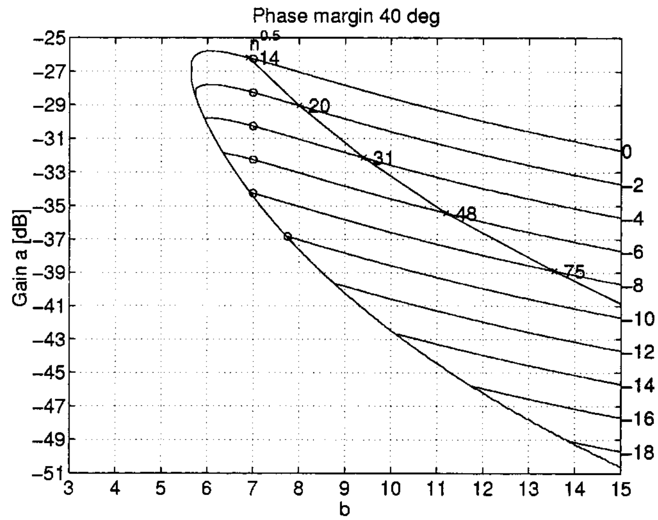

Fig. 6. Modified ϕ-curves for phase margin 40° and gain uncertainties from 0 dB to 18 dB every 2 dB, also shown are $a_0(n)$, $b_0(n)$ and the points n_0 at the intersections, marked $\times$. The points marked $\circ$ are the points that minimize $\sigma_e^2(1,0,1)$ on the modified ϕ-curve.

with phase error $\sigma_e = 3.6°$. This result is better by 7.7 dB if we restrict ourselves to a second-order design (see Section IV-A-I).

C. The Solution for $\phi_\theta(\omega) \propto \omega^{-4}$ and White Noise

Since the near-optimal design method described above is quite complex, we have chosen a very common case of parameters and solved it fully. The result is a cookbook for PLL design with delay, which can be used if the phase noise spectrum can be approximated as $\Phi_\theta(\omega) \propto \omega^{-4}$ and if the margins assumed here are appropriate. Let

$$\Phi_\theta(\omega) = \frac{B_0^2}{\omega^4} \text{ and } \Phi_n(\omega) = N_0 \tag{24}$$

where B_0 is constant and N_0 is the usual white noise density. Equation (5) gives

$$\begin{aligned}\sigma_e^2 =& \frac{1}{2\pi}\int_{-\infty}^{\infty}\left|\frac{A\tilde{F}(j\omega)}{A\left(1+e^{-j\omega T}A\tilde{F}(j\omega)\right)}\right|^2 N_0 d\omega \\ &+ \frac{1}{2\pi}\int_{-\infty}^{\infty}\left|\frac{1}{1+e^{-j\omega T}A\tilde{F}(j\omega)}\right|^2\frac{B_0^2}{\omega^4}d\omega \\ =& \frac{N_0}{2\pi T}\left(\int_{-\infty}^{\infty}\left|\frac{A\tilde{F}\frac{j\Omega}{T}}{A\left(1+e^{-j\Omega}A\tilde{F}\frac{j\Omega}{T}\right)}\right|^2\right. \\ &\left.+\int_{-\infty}^{\infty}\left|\frac{1}{1+e^{-j\Omega}A\tilde{F}\frac{j\Omega}{T}}\right|^2\frac{B_n^2}{\Omega^4}\right)d\Omega\end{aligned} \tag{25}$$

where

$$B_n^2 = \frac{B_0^2T^4}{N_0}, \quad \Omega = \omega T.$$

Clearly $\tilde{F}(j\Omega/T)$, which minimizes σ_e^2 of (25), depends only on B_n, in the sense that if $\tilde{F}(s)$ minimizes σ_e^2 for $T=1$ then $\tilde{F}(sT_0)$ minimizes σ_e^2 for $T=T_0$; moreover, for given B_n^2

$$\sigma_e^2(T,N_0)=\frac{N_0}{T}\sigma_e^2 \quad (T=1,\ \ N_0=1). \tag{26}$$

We therefore use the design technique developed here to present a PLL designer $\tilde{F}(s)$'s which suits different B_n^2's. We limit ourselves to $\tilde{F}(s)$'s which have only two free integrators, phase margin 40° and uncertainty $A\in[A_1,2A_1]$ (which is equivalent to a phase margin of 40° and gain margin 16 dB which is in the reasonable PLL operation range).

By checking many cases, it was found that for $B_n\le 0.02$ the optimal solution satisfies the margin specifications; therefore, the case where $B_n\le 0.02$ is not an interesting case here. On the other hand, as B_n increases, $\tilde{F}(s)$ converges to a single solution. We found that $\tilde{F}(s)$ approximately stays constant for $B_n\ge 0.15$. Our designs are summarized below normalized for $A_1=1$:

$$\tilde{F}(B_n=0.02)=\frac{0.22(s+4)^2(s+0.091)}{s^2(s^2+8.0s+19.4)}$$
$$\tilde{F}(B_n=0.03)=\frac{0.29(s+1.0)(s+0.46)(s+0.1094)}{(s+1.8)(s+0.36)s^2}$$
$$\tilde{F}(B_n=0.04)=\frac{0.34(s+1.36)(s+0.43)(s+0.11)}{(s+2.5)(s+0.36)s^2}$$
$$\tilde{F}(B_n=0.05)=\frac{1.09(s+3.48)(s+2.6)(s+0.43)(s+0.106)}{(s+13.7)(s+3.7)(s+0.30)s^2}$$
$$\tilde{F}(B_n=0.06)=\frac{0.78(s+5.08)(s+0.46)(s+0.087)(s^2+5.8s+8.7)}{s^2(s+7.6)(s+0.28)(s^2+7.8s+22.0)}$$
$$\tilde{F}(B_n=0.08)=\frac{0.68(s+0.078)(s^2+1.57s+0.84)}{(s+4.6)(s+0.34)s^2}$$
$$\tilde{F}(B_n=0.1)=\frac{0.79(s+0.17)(s+0.035)(s^2+1.77s+1.63)}{(s+4.81)(s+1.0)(s+0.055)s^2}$$
$$\tilde{F}(B_n=0.15)=\frac{0.79(s+0.17)(s+0.035)(s^2+1.77s+1.63)}{(s+4.8)(s+1.0)(s+0.055)s^2}.$$

The σ_e^2 values for $T=1$ as a function of B_n are given in Fig. 7. Note that, for given spectrum structure [especially (24)] as $B_n\to\infty$ and $N_0\to 0$, $\tilde{F}(s)$ converges to its value for $N_0=0$. Based on the above results, a step-by-step procedure for delayed PLL design is as follows.

1) Calculate B_n.
2) If $B_n\le 0.02$, use a PI loop filter or any optimal existing technique.
3) If $B_n\ge 0.15$, the open loop is $\tilde{F}(sT)$ using $\tilde{F}(B_n=0.15)$.
4) If $0.02<B_n<0.15$, choose the closest $\tilde{F}(s)$ from the table above, then use $\tilde{F}(sT)$.
5) Calculate σ_e^2 via Fig. 7 and (26).

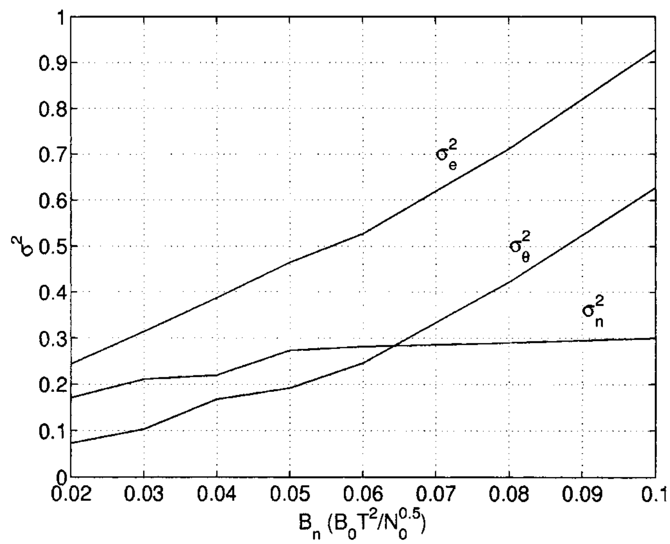

Fig. 7. σ_e^2, its noise contribution σ_n^2, and its phase noise σ_θ^2 versus B_n.

IV. Loop Filters Having a PI Form

A *restricted order* loop filter is a loop filter which has less poles and zeros than the optimal loop filter. There are three reasons for using a restricted order loop filter: 1) reduction of computation effort in real time; 2) the design of a restricted order loop filter may be simpler and faster; and 3) the restricted order loop filter can be close enough to the optimal loop filter. The drawback of using a restricted order loop filter is when 3) is not satisfied, that is, it produces too much error compared to a nonrestricted order design.

The PLL open loop when the loop filter is PI can be written as follows:

$$L(s)=\frac{e^{-sT}}{sT}\frac{a(1+bsT)}{sT} \tag{27}$$

and the two parameters to design are a and b. Since $L(j\omega)$ can be written as a function of ωT, the range of $L(j\omega)$ for all real ω does not depend on T. Therefore, if margin specification of the form

$$\left|\frac{1}{1+L(j\omega)}\right|\le\delta, \quad \forall\,\omega \tag{28}$$

is satisfied for some T, it is satisfied for any T. This normalizes the problem for the margin specification for all T, and $T=1$ will be picked in the following. Let us now denote by ω_0 a frequency for which (28) is satisfied with equality. Explicitly there exists ω_0 such that

$$\left|1+\frac{e^{-sT}}{sT}\frac{a(1+bsT)}{sT}\right|_{s=j\omega_0}=\frac{1}{\delta}$$

and ω_0 is an extremum point of $|1+L(j\omega)|$. Hence

$$a^2\frac{1+b^2\omega_0^2}{\omega_0^4}-2a\frac{\cos(\omega_0)+b\omega_0\sin(\omega_0)}{\omega_0^2}+1-\frac{1}{\delta^2}=0 \tag{29}$$

$$\frac{\partial}{\partial\omega}\left(a^2\frac{1+b^2\omega^2}{\omega^4}-2a\frac{\cos(\omega)+b\omega\sin(\omega)}{\omega^2}+1\right)_{\omega=\omega_0}=0. \tag{30}$$

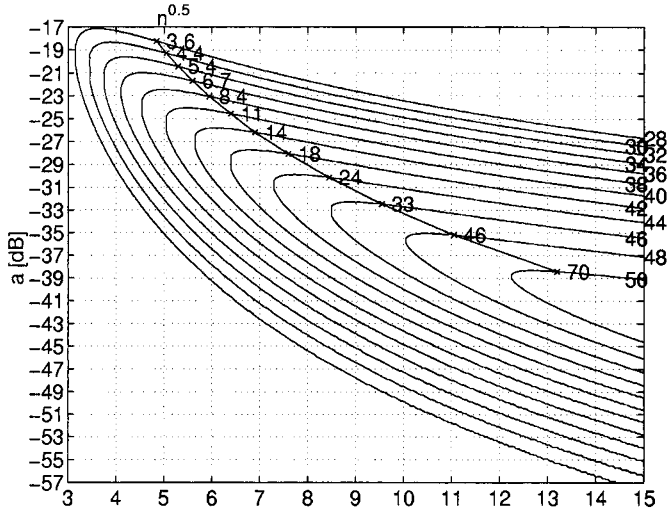

Fig. 8. (a, b) curves for different phase margins, marked on its right side. Also, the location of (a, b)'s which minimize σ_e^2 on the ϕ-curves and their $\sqrt{n}$ values.

From (30), we have (31), shown at the bottom of the page. The solution of (29) and (31), for given δ, as a function of ω_0 is a curve $(a(\omega_0), b(\omega_0))$ in R^2. These curves are functions of the parameter δ which dictates phase margin ϕ according to (3); we shall therefore call them the δ-curves or ϕ-curves. These curves are depicted in Fig. 8. Clearly, these curves cannot intersect. Moreover, if we denote by D_ϕ the region inside the curve of phase margin ϕ, then $D_{\phi_1} \subset D_{\phi_2}$ if $\phi_1 < \phi_2$ (equivalently, if $\delta(\phi_1) > \delta(\phi_2)$). Therefore, any (a, b) curve splits R^2 into two regions, D_ϕ in which inequality (28) is satisfied and its complement in which inequality (28) is not satisfied. For example, if a phase margin of 40° is required (which is equivalent to $\delta = 3.3$ dB and 10 dB gain margin), then for $b = 15$ the allowed values for a are $-50.5 \le a \le -31.8$, and for $b = 10$, $-42.5 \le a \le -28.5$.

The extension to gain uncertainty is now straightforward: if it is known that the gain can increase by r dB then the allowed region, D_ϕ^r, is the intersection of D_ϕ and the region D_ϕ shifted down by r dB (to protect against possible gain increase of r dB). For example, if phase margin of 40° is required, $b = 15$, and $r = 14$ dB, then -56.5 dB $\le a \le -45.8$ dB, and if $b = 10$ then -42.5 dB $\le a \le -42.5$ dB, that is, no tolerance in a. Therefore, if $r > 14$ dB, $b \le 10$ cannot be used. The maximum gain range a PI loop filter can tolerate as a function of the phase margin for different values of b can easily be retrieved from Fig. 8. For example, at 40° and $b = 15$, the gain uncertainty range can be 19 dB, that is, in order to handle 19 dB uncertainty with $b = 15$, the chosen gain must be $a = (-28.5 - 19)$ dB and the gain margin of $L(s)$ is between 10 dB for the maximum gain and 29 dB for the minimum gain. If, for example, the phase margin is 42° and the gain range is 10 dB, then $b \ge 9$ must be picked in order to satisfy inequality (28) by all possible $L(s)$ which suffers from 10 dB gain uncertainty.

Now let us suppose that σ_e^2, where a PI loop filter is used, has a unique minimum, which does not satisfy given margin constraints ϕ. Then, the (a, b) pair which minimizes σ_e^2 subjected to the margin constraint ϕ must lie on the surface of D_ϕ, that is, on the ϕ-curve. In that case, the design process reduces into an extremum problem with a single parameter and single minimum as follows.

1) Pick the curve (a, b) from Fig. 8 for the chosen phase margin specification, and modify it to the appropriate gain uncertainty as described above.
2) Find along the (a, b) curve picked in 1 the extremum of

$$\begin{aligned}\sigma_e^2(a,b) =& \frac{1}{2\pi}\int_{-\infty}^{\infty}\left|\frac{e^{-sT}a(1+bsT)}{(sT)^2+e^{-sT}a(1+bsT)}\right|^2_{s=j\omega} \\ &\times \Phi_n(\omega)d\omega \\ &+\frac{1}{2\pi}\int_{-\infty}^{\infty}\left|\frac{(sT)^2}{(sT)^2+e^{-sT}a(1+bsT)}\right|^2_{s=j\omega} \\ &\times \Phi_\theta(\omega)d\omega \\ =& \frac{1}{2\pi T}\int_{-\infty}^{\infty}\left|\frac{a(1+bs)}{s^2+e^{-s}a(1+bs)}\right|^2_{s=j\omega} \\ &\times \Phi_n\left(\frac{\omega}{T}\right)d\omega \\ &+\frac{1}{2\pi T}\int_{-\infty}^{\infty}\left|\frac{s^2}{s^2+e^{-s}a(1+bs)}\right|^2_{s=j\omega} \\ &\times \Phi_\theta\left(\frac{\omega}{T}\right)d\omega. \end{aligned} \tag{32}$$

3) The PI optimal loop filter will then be

$$F(s) = \frac{a(1+bTs)}{A_1T^2s}$$

where $AP = Ae^{-sT}/s$ and $A \in [A_1, A_2]$.

A. The PI Solution for $\phi_\theta(\omega) \propto \omega^{-4}$ and White Noise

We treat here the case

$$\Phi_\theta(\omega) = \frac{B_0^2}{\omega^4} \text{ and } \Phi_n(\omega) = N_0 \tag{33}$$

where B_0 is a constant and N_0 is the usual white noise density. Substituting into (32) gives

$$\begin{aligned}\sigma_e^2 =& \frac{1}{2\pi T}\int_{-\infty}^{\infty}\left|\frac{a(1+bs)\sqrt{N_0}}{s^2+e^{-s}a(1+bs)}\right|^2_{s=j\omega}d\omega \\ &+\frac{1}{2\pi T}\int_{-\infty}^{\infty}\left|\frac{\frac{s^2B_0T^2}{\omega^2}}{s^2+e^{-s}a(1+bs)}\right|^2_{s=j\omega}d\omega.\end{aligned} \tag{34}$$

Clearly

$$\sigma_e^2(T, N_0, B_0) = B_0^2T^3\sigma_e^2(1, n, 1), \quad n = \frac{N_0}{B_0^2T^4} \tag{35}$$

thus the (a, b) pair which minimizes σ_e^2 depends only on the single parameter n. Note that $n = B_n^{-2}$ is defined in (26) but

$$a = \frac{\sin(\omega_0) - b\sin(\omega_0) - b\omega_0\cos(\omega_0) + \frac{2(\cos(\omega_0)+b\omega_0\sin(\omega_0))}{\omega_0}}{\frac{2}{\omega_0^3}+\frac{b^2}{\omega_0}} \tag{31}$$

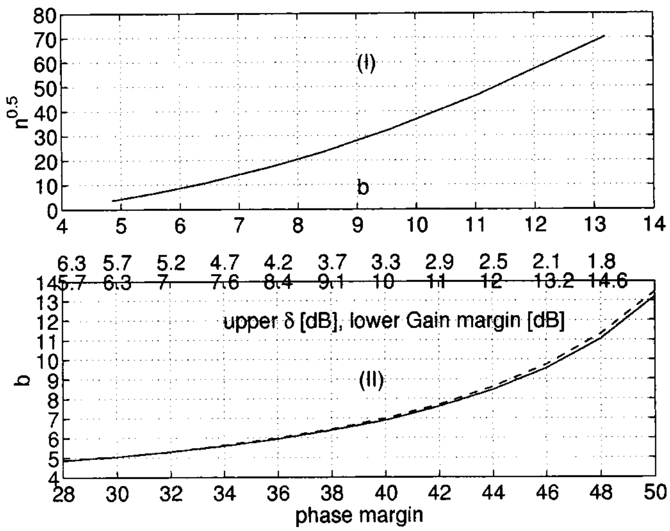

Fig. 9. (a) $\sqrt{n_0}$ as a function of b_0. (b) $b_0(\phi)$ (solid line) (a_0 can be picked from Fig. 8 and b which minimizes $\sigma_e^2(1, n = 0, 1)$ on the same ϕ-curve (dashed line).

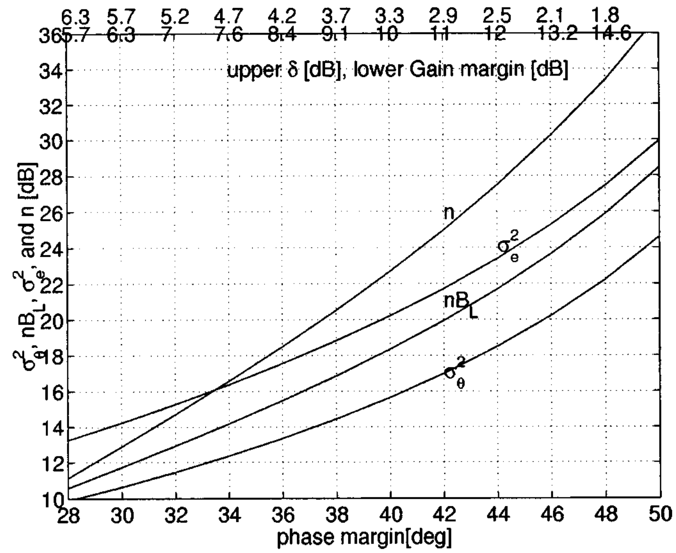

Fig. 10. The phase error σ_e^2, the phase noise contribution σ_θ^2, the thermal noise contribution $n_0 B_L$ and n_0 versus phase margin.

we use n for clarity. Let $\{a_0(n), b_0(n)\}$ be the point that minimizes σ_e^2 as a function of n. The curve $\{a_0(n), b_0(n)\}$ is plotted on top of the ϕ-curves in Fig. 8. Let us further denote the intersection point of the curve $\{a_0(n), b_0(n)\}$ with a ϕ-curve by $a_0(\phi)$, $b_0(\phi)$, and $n_0(\phi)$. For example, if a phase margin of 40° is required assuming no gain uncertainty, then $\sqrt{n_0} = 13.8$, $a_0 = -26.3$ dB and $b_0 = 7.8$. $a_0(n)$, $b_0(n)$ were calculated as follows: first σ_e^2 in (34) is written as

$$\sigma_e^2 = nB_L + \sigma_\theta^2.$$

Hence, $a_0(n)$, $b_0(n)$ minimizes σ_e^2 for some n if

$$n = -\frac{\partial\sigma_\theta^2/\partial a}{\partial B_L/\partial a} \text{ and } n = -\frac{\partial\sigma_\theta^2/\partial b}{\partial B_L/\partial b}. \tag{36}$$

The two partial derivative ratios in (36) where calculated along each of the ϕ-curves in Fig. 8 and it was found that they have a unique intersection, whose n value is written on its ϕ-curve in Fig. 8. This proves, numerically, that $\sigma_e^2(n)$ has a unique minimum. Moreover, we observe that $n(\phi)$ is a monotonicaly increasing function of ϕ. The same results are depicted in Fig. 9 which includes a graph of n_0 as a function of b_0 and a graph of $b_0(\phi)$.

Fig. 9(b) also shows b which minimizes $\sigma_e^2(1, n = 0, 1)$ on the ϕ-curve. Since the two curves in Fig. 9(b) almost coincide, and the solution for constrained minimization of σ_e^2 for $n = 0$ must lie on the ϕ-curve, the $a_0(\phi)$, $b_0(\phi)$ pair, for a very good approximation, minimize $\sigma_e(1, n_1, 1)$ for any $n_1 \leq n_0(\phi)$. But this will not be the case if uncertainty is introduced. Fig. 6 depicts modified ϕ-curves for a phase margin of 40° and uncertainties between 0 dB and 18 dB every 2 dB. $\sqrt{n_0}$ at the intersection of $a_0(n)$, $b_0(n)$ with the modified ϕ-curve is marked on each curve. For $n_1 < n_0$, the (a, b) pairs which minimize $\sigma_e(1, n_1, 1)$ on the modified ϕ-curve move along that curve toward the point marked ∘ which is the minimum point for $n_1 = 0$. Finally, Fig. 10 depicts $\sqrt{n}\sigma_n$, σ_θ, σ_e, and $\sqrt{n}$ on the point $a_0(\phi)$, $b_0(\phi)$ as a function of ϕ.

1) Example 3.2—Continuation: For 40° phase margin and 6 dB gain margin, use Fig. 6 to get $a = -32.3$ dB and $b = 7$, then

$$F(s) = 0.0243\frac{7Ts + 1}{T^2s^2}, \text{ whose } \sigma_e = 8.7°.$$

2) Tradeoff Amongst Restricted Order, Delay Time, and Phase Noise: The first tradeoff is based on (34) which states that when N_0 is small enough then the thermal noise contribution in (35) is neglected and therefore $\sigma_e^2 \propto B_0^2 T^3$.

The next tradeoff we are interested in is by how much σ_e^2 can be reduced by a loop filter designed by the method of Section III compared to a PI loop filter. The answer provided here is based on an example whose parameters are: $\Phi_\theta = 50^2/\omega^4$, Φ_n can be neglected, open loop delay $T = 0.01$, and gain uncertainty A in the interval $A \in [1, 2.5]$, that is, 8 dB uncertainty. The margin specification is of the form $|1 + L|^{-1} < 3.3$ dB, which guarantees a 40° phase margin and 10-dB gain margin for $A = 2.5$ and 18 dB for $A = 1$.

Using Fig. 6 for 8-dB uncertainty, $a = -34.3$ dB and $b = 7$. For that PI loop filter, $\sigma_e^2 = 0.57$. Using the suboptimal methodology described herein, the loop filter is

$$F_r(s) = 32.7\frac{(s + 120)(s + 570)(s^2 + 11.4s + 38)}{s^2(s + 300)(s + 28)}$$

for which $\sigma_e^2 = 0.28$. This figure is half of that figure when an optimal PI loop filter is used. By (35), it is equivalent to a 3-dB reduction of the phase noise spectral density or 25% in the delay time.

V. Conclusion

We have presented a design method for near-optimal PLL taking into consideration the phase noise, the thermal noise, the undesired but unavoidable loop delay caused by delayed decisions, and margins for protection from gain uncertainty and insuring good step response. The method is general and can be used with any PLL. We find its main application in carrier tracking since a wide-loop bandwidth is required to track the phase noise. We do not limit the loop order to be second order, and we demonstrate a large performance gain with respect to a well-designed second-order loop.

REFERENCES

[1] A.-N. Premji and D. P. Taylor, "Receiver structures for multi-h signaling formats," *IEEE Trans. Commun.*, vol. 35, pp. 439–442, Apr. 1987.

[2] J. R. Bary and J. M. Kahn, "Carrier synchronization for homodyne and heterodyne detection of optimal quadriphase-shift keying," *J. Lightwave technol.*, vol. 10, pp. 1939–1951, Dec. 1992.

[3] J. W. M. Bergmans, "Effect of loop delay on stability of discrete-time PLL," *IEEE Trans. and Syst. I*, vol. 42, pp. 229–231, Apr. 1995.

[4] *Quantitative Feedback Theory Toolbox*, The MathWorks Inc, Natick, MA, 1994.

[5] Y. Chait and O. Yaniv, "Multi-input/single-output computer-aided control design using the quantitative feedback theory," *Int. J. Robust Nonlinear Contr.*, vol. 3, pp. 47–54, 1993.

[6] R. W. Chang and R. Srinivasagopalan, "Carrier recovery for data communication systems with adaptive equalization," *IEEE Trans. Commun.*, vol. COM-28, pp. 1142–1153, Aug. 1980.

[7] J. D'Azzo and C. H. Houpis, *Linear Control System Analysis and Design Conventional and Modern*, 3rd ed. New York: McGraw-Hill, 1988.

[8] J. C. Doyle, B. A. Francis, and A. R. Tannenbaum, *Feedback Control Theory*. New York: Macmillan, 1992.

[9] F. Bernard, *Advanced Control System Design*. Englewood Cliffs, NJ: Prentice-Hall, 1966.

[10] M. A. Grany, W. C. Michie, and M. J. Fletcher, "The performance of optical phase-locked loops in the presence of nonnegligible loop propagation delay," *J. Lightwave technol.*, vol. LT-5, pp. 592–597, Apr. 1987.

[11] J. K. Holmes, *Coherent Spread Spectrum Systems*. New York: Wiley, 1982.

[12] I. Horowitz, *Quantitative Feedback Design Theory (QFT)*. Boulder, CO: QFT Publications, 1992.

[13] ——, "Invited paper—Survey of quantitative feedback theory (QFT)," *Int. J. Control*, vol. 53, no. 2, pp. 255–291, 1991.

[14] W. C. Lindsey, *Synchronization Systems in Communication and Control*. Englewood Cliffs, NJ: Prentice-Hall, 1972.

[15] A. J. Macdonald and J. B. Anderson, "PLL synchronization for coded modulation," in *Int. Comm. Conf. ICC'91*, 1991, pp. 1708–1712.

[16] G. H. Martin, "Designing phase-locked loops," *R.F Design*, vol. 20, no. 5, p. 56, 1997.

[17] S. Moride and H. Sari, "Effect of loop delay on the pull-in range of generalized second-order phase locked loops," in *ICC*, Seattle, WA, June 1987, pp. 1041–1045.

[18] N. Seiji and K. Iwashita, "PLL propagation delay-time influence on linewidth requirements of optical PSK homodyne detection," *J. Lightwave Technol.*, vol. 9, pp. 1367–1375, Oct. 1991.

[19] A. N. Premji and D. P. Taylor, "Receiver structures for multi-h signaling formats," *IEEE Trans. Commun.*, vol. 35, no. 4, pp. 439–450, 1987.

[20] S. Hikmet, S. Moridi, L. Desperben, and P. Vandamme, "Baseband equalization and carrier recovery in digital radio systems," *IEEE Trans. Commun.*, vol. COM-35, pp. 319–327, Mar. 1987.

[21] U. Shaked, "A general transfer function approach to linear stationary filtering and steady state optimal control problems," *Int. J. Control*, vol. 4, no. 6, pp. 741–770, 1976.

[22] S. J. Simmons and P. J. McLane, "Low-complexity carrier phase tracking decoders for continuous phase modulations," *IEEE Trans. Commun.*, vol. 33, pp. 1285–1290, Dec. 1995.

[23] U. Gottfried, "Channel coding with multilevel/phase signals," *IEEE Trans. Inform. Theory*, vol. IT-28, pp. 55–67, Jan. 1982.

Oded Yaniv (M'88–SM'99) was born in Israel in 1950. He received the B.Sc. degree in physics and mathematics from the Hebrew University of Jerusalem in Israel in 1974, and the M.Sc. degree in physics and the Ph.D. degree in applied mathematics from the Weizmann Institute of Science, Rehovot, Israel, in 1978 and 1984, respectively.

During the years 1978–1980 and 1984–1988, he was employed at several industries in Israel as a physicist and control engineer. Since 1988, he has been with the Faculty of Engineering, Department of Electrical Engineering—Systems, Tel Aviv University, Tel Aviv, Israel. His main research field is robust synthesis of MIMO feedback systems.

Dan Raphaeli (S'93–M'95–SM'99) was born in Israel in 1967. He received the B.Sc. degree in electrical and computer engineering from Ben Gurion University, Israel, in 1986 and the M.S. and Ph.D. degrees in electrical engineering from the California Institute of Technology, Pasadena, in 1992 and 1994, respectively.

From 1986 to 1991, he was a research member at the Electronic Research Institute of the Israel Defense Ministry, where he was involved in the development of many advanced communication and signal processing projects. From 1992 to 1994, he was with the Jet Propulsion Laboratory, Pasadena, CA, where he was involved in research on communication systems for future spacecrafts. Since 1994, he has been an Assistant Professor with the Department of Electrical Engineering-Systems, Tel Aviv University, Tel Aviv, Israel. He is a founder of Itran Communications and a professional consultant to industry in Modem design and DSP. His research subjects include modulation/demodulation, turbo codes, coding and decoding algorithms, spread spectrum, mobile communication, synchronization, equalization, and digital signal processing.